

HC-GLAD: Dual Hyperbolic Contrastive Learning for Unsupervised Graph-Level Anomaly Detection

Yali Fu*
Jilin University
Changchun, China
fuy23@mails.jlu.edu.cn

Jindong Li*
Jilin University
Changchun, China
jldi21@mails.jlu.edu.cn

Jiahong Liu
The Chinese University of Hong Kong
Hong Kong SAR, China
jiahong.liu21@gmail.com

Qianli Xing
Jilin University
Changchun, China
qianlixing@jlu.edu.cn

Qi Wang[†]
Jilin University
Changchun, China
Engineering Research Center of
Knowledge-Driven Human-Machine
Intelligence, Ministry of Education,
China
qiwang@jlu.edu.cn

Irwin King
The Chinese University of Hong Kong
Hong Kong SAR, China
king@cse.cuhk.edu.hk

ABSTRACT

Unsupervised graph-level anomaly detection (UGAD) has garnered increasing attention in recent years due to its significance. Most existing methods that rely on traditional GNNs mainly consider pairwise relationships between first-order neighbors, which is insufficient to capture the complex high-order dependencies often associated with anomalies. This limitation underscores the necessity of exploring high-order node interactions in UGAD. In addition, most previous works ignore the underlying properties (e.g., hierarchy and power-law structure) which are common in real-world graph datasets and therefore are indispensable factors in the UGAD task. In this paper, we propose a novel Dual Hyperbolic Contrastive Learning for Unsupervised Graph-Level Anomaly Detection (HC-GLAD in short). To exploit high-order node group information, we construct hypergraphs based on pre-designed gold motifs and subsequently perform hypergraph convolution. Furthermore, to preserve the hierarchy of real-world graphs, we introduce hyperbolic geometry into this field and conduct both graph and hypergraph embedding learning in hyperbolic space with the hyperboloid model. To the best of our knowledge, this is the first work to simultaneously apply hypergraph with node group information and hyperbolic geometry in this field. Extensive experiments on 13 real-world datasets of different fields demonstrate the superiority of HC-GLAD on the UGAD task. The code is available at <https://github.com/Yali-F/HC-GLAD>.

KEYWORDS

Graph-level Anomaly Detection, Hyperbolic Representation Learning, Unsupervised Learning, Graph Neural Networks

1 INTRODUCTION

Graph-level anomaly detection helps uncover anomalous behaviors hidden within complex graph structures, which has been widely applied in various fields, including social network analysis, bioinformatics, and network security [23, 26, 27]. Unlike traditional anomaly

*Equal contributions.

[†]Corresponding author.

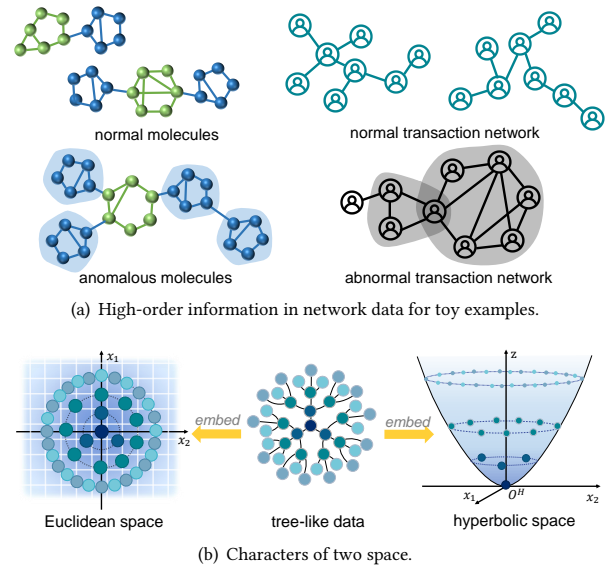


Figure 1: (a) Normal molecular graphs usually have 1-2 node groups in blue areas, while abnormal ones have 3-4. Normal financial transaction networks show simple patterns, while abnormal ones show chaotic circular or cross-transactions in gray areas; (b) With an exponential increase of nodes in tree-like data, Euclidean space is difficult to embed nodes separately. In contrast, hyperbolic space, which can be regarded as a continuous version of the tree, can still maintain certain distances between the embedded nodes.

detection methods that focus on individual data points or samples, graph-level anomaly detection focuses on the overall structure, topology, or features of the entire graph. Recently, there has been a growing interest in unsupervised graph-level anomaly detection (UGAD) as it offers an advantage by not relying on labeled data, rendering it applicable across various real-world scenarios. Despite

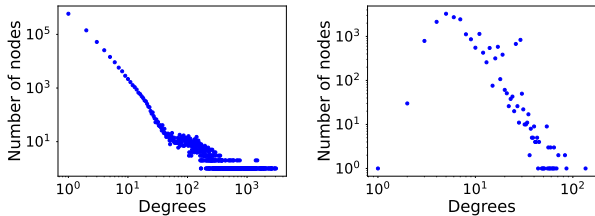


Figure 2: Degree distributions of dataset REDDIT-B (on the left) and IMDB-B (on the right).

the considerable research and exploration already conducted in this area [19, 22, 34, 56], there are still several issues that need to be further explored.

Firstly, most existing UGAD methods using GNNs treat edges and nodes as fundamental units for message passing [56], relying solely on pairwise relationships to capture key patterns. However, real-world networks often involve group interactions among multiple nodes, particularly in protein-protein interactions (PPI), molecular complexes, and delocalized bonds among multiple atoms [8, 9]. In some cases, anomalous graphs arise from these complex interactions among multiple nodes, exhibiting patterns significantly different from normal graphs. As shown in Figure 1(a), the decisive factor in determining whether a molecule is anomalous lies in distinct groups connected to the central group: while normal molecular graphs typically involve fewer external groups, anomalous ones exhibit more complex group structures [23]. Similarly, abnormal financial transactions are characterized by more intricate transaction patterns, where anomalies often stem from irregular or convoluted interactions among multiple accounts, differing from the straightforward patterns in normal transactions. There is an urgent need to holistically consider such complex group interactions to capture key patterns for anomaly detection.

Secondly, the majority of current methods are based on GNNs established in Euclidean space [22, 27], but the dimensionality of Euclidean space brings a fundamental limitation on its ability to represent complex networks [32]. It has been demonstrated that numerous real-world datasets exhibit characteristics akin to those of complex networks, including degree power-law distribution as shown in Figure 2, which embodies latent tree-like hierarchical structure [6, 38]. In such tree-like data, the number of nodes has an exponential growth trend. For instance, the total number of nodes is $2^{(h+1)} - 1$ (h is the height of the tree) in a full binary tree. Nevertheless, flat Euclidean space whose volume grows polynomially cannot embed latent hierarchies without suffering from high distortion, as shown in Figure 1(b). Therefore, it is necessary to employ a new paradigm or space to exploit the latent hierarchical information in UGAD.

Based on the aforementioned challenges and analysis, we propose a novel Dual Hyperbolic Contrastive Learning for Unsupervised Graph-Level Anomaly Detection framework, namely HC-GLAD. In concrete, for the first challenge, we introduce hypergraph to naturally capture high-order structures beyond pairwise relationships. The anomaly-aware hypergraph is constructed based on pre-designed gold motifs. Compared to traditional graph structures, hyperedges in hypergraphs can connect multiple nodes, and hypergraph convolution enables message propagation in a broader

context, yielding more comprehensive feature representations. This approach can not only capture local node interactions but also integrate global information through hyperedges, identifying high-order structures that deviate from normal patterns, thereby improving the accuracy of anomaly detection. For the second challenge, we incorporate hyperbolic geometry into UGAD. The curved hyperbolic space can be seen as a continuous version of the tree with exponential growth [52], allowing it to naturally retain the rich hierarchical information in graph data. Also, under the same radius, the hyperbolic space can accommodate more nodes for informative embeddings as shown in Figure 1(b). Specifically, we utilize the hyperboloid model to preserve the latent hierarchical information and conduct both graph and hypergraph embedding in hyperbolic space. Our major contributions are summarized as follows:

- We propose a novel dual hyperbolic contrastive learning for the unsupervised graph-level anomaly detection framework (HC-GLAD). To the best of our knowledge, this is the first work to simultaneously introduce hypergraph exploiting node group information and hyperbolic geometry to the unsupervised graph-level anomaly detection task.
- We utilize hypergraphs to explore node group information based on pre-designed gold motifs. In addition, we employ hyperbolic geometry to leverage latent hierarchical information and accomplish achievements that cannot be attained in Euclidean space. The advantages of hypergraph learning, hyperbolic learning, and contrastive learning are integrated into a unified framework to jointly improve model performance.
- We conduct extensive experiments on 13 real-world datasets, demonstrating the effectiveness and superiority of HC-GLAD for unsupervised graph-level anomaly detection.

2 RELATED WORK

2.1 Graph-Level Anomaly Detection

In the context of graph data analysis, the objective of graph-level anomaly detection is to discern abnormal graphs from normal ones, wherein anomalous graphs often signify a minority but pivotal patterns [28]. Nowadays, there are numerous methods that explore graph-level anomalies in graphs. OCGIN [62] is the first representative model, and it integrates the one-class classification and graph isomorphism network (GIN) [48] into the graph-level anomaly detection. OCGTL [36] integrates the strengths of deep one-class classification and neural transformation learning. GLocalKD [27] implements joint random distillation to detect both locally anomalous and globally anomalous graphs by training one graph neural network to predict another graph neural network. GOOD-D [22] introduces perturbation-free graph data augmentation and performs hierarchical contrastive learning to detect anomalous graphs based on semantic inconsistency in different levels. TUAF [56] builds triple-unit graphs and further learns triple representations to simultaneously capture abundant information on edges and their corresponding nodes. CVTGAD [19] applies transformer and cross-attention into UGAD, directly exploiting relationships across different views. SIGNET [23] proposes a multi-view subgraph information bottleneck framework and further infers anomaly scores and provides subgraph-level explanations.

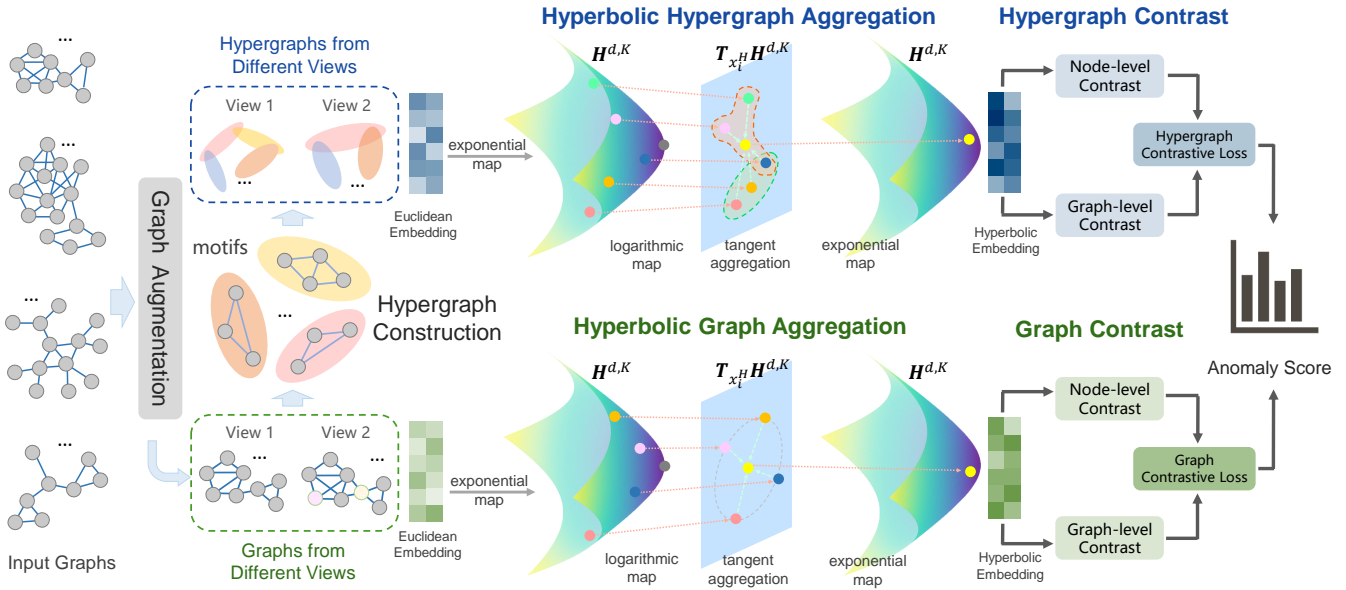


Figure 3: The overall framework of HC-GLAD. Firstly, the input graphs undergo data augmentation in Euclidean space, obtaining two augmented views and forming the graph channel below. Secondly, based on pre-designed gold motifs, we construct hypergraphs from the augmented graphs, forming the hypergraph channel above. Thirdly, we perform the aggregation operation for graph and hypergraph channel in hyperbolic space, obtaining final hyperbolic embeddings used for calculating multi-level contrastive loss. Lastly, graph and hypergraph contrastive losses are employed to calculate graphs’ anomaly scores.

2.2 Hyperbolic Learning on Graphs

Hyperbolic learning has attracted massive attention from the graph fields such as recommendation systems, node classification, and molecular learning due to its superior geometry property (i.e., its volume increases exponentially in proportion to its radius) of hyperbolic space compared to Euclidean space [50, 51]. HGNN (hyperbolic graph neural network) [21] generalizes the graph neural networks to Riemannian manifolds and improves the performance of the full-graph classification task. It fully utilizes the power of hyperbolic geometry and demonstrates that hyperbolic representations are suitable for capturing high-level structural information. HGCN (hyperbolic graph convolutional neural network) [7] leverages both the expressiveness of GCNs and hyperbolic geometry. κ -GCN [3] presents an innovative expansion of GCNs to encompass stereographic models with both positive and negative curvatures, thereby offering a unified approach. HAT (hyperbolic graph attention network) [58] proposes the hyperbolic multi-head attention mechanism to acquire robust node representation of graph in hyperbolic space and further improves the accuracy of node classification. LGCN [59] introduces a unified framework of graph operations on the hyperboloid (i.e., feature transformation and non-linearity activation), and proposes an elegant hyperbolic neighborhood aggregation based on the centroid of Lorentzian distance. HRCF [52] designs a geometric-aware hyperbolic regularizer to boost the optimization process by the root alignment and origin-aware penalty, and it enhances the performance of a hyperbolic-powered collaborative filtering. HyperIMBA [11] explores the hierarchy-imbalance issue on hierarchical structure and captures the implicit hierarchy of graph nodes by hyperbolic geometry.

2.3 Hypergraph Learning

Due to the capability and flexibility in modeling complex correlations of graph data, hypergraph learning has earned more attention from both academia and industry [13]. Hypergraphs naturally depict a wide array of systems characterized by group relationships among their interacting parts [2]. HGNN (hypergraph neural network) [10] designs a hyperedge convolution operation and encodes high-order data correlation in a hypergraph structure. HyperGCN [49] utilizes tools from the spectral theory of hypergraphs and introduces a novel way to train GCN for semi-supervised learning and combinatorial optimization tasks. HGNN⁺ [12] introduces "hyperedge groups" to capture high-order correlations in multi-modal data and uses an adaptive fusion strategy to integrate them into a unified hypergraph. This allows the model to better represent complex relationships across different data types. DHCF [16] constructs two hypergraphs (i.e., user and item hypergraph) and introduces a jump hypergraph convolution (jHConv) to enhance collaborative filtering recommendation performance. HHGR [57] builds user-level and group-level hypergraphs and employs a hierarchical hypergraph convolution network to capture complex high-order relationships within and beyond groups, thus improving the performance of group recommendation. DH-HGCN [15] utilizes both a hypergraph convolution network and homogeneity study to explicitly learn high-order relationships among items and users to enhance multiple social recommendation performance. HCCF [47] designs a hypergraph-enhanced cross-view contrastive learning architecture to jointly capture local and global collaborative relations in the recommender system.

An extensive review of the literature is included in Appendix A.

3 PRELIMINARIES

3.1 Hyperboloid Manifold

Hyperbolic space, defined by its constant negative curvature, diverges from the flatness of Euclidean geometry. The hyperboloid manifold is often favored for its numerical stability, making it a popular choice in hyperbolic geometry applications [33].

Definition 3.1 (Minkowski Inner Product). The inner product $\langle \mathbf{x}, \mathbf{y} \rangle_{\mathcal{L}}$ for vectors $\mathbf{x}, \mathbf{y} \in \mathbb{R}^{d+1}$ is defined by the expression $\langle \mathbf{x}, \mathbf{y} \rangle_{\mathcal{L}} = -x_0y_0 + \sum_{i=1}^d x_iy_i$.

Definition 3.2 (Hyperboloid Manifold). A d -dimensional hyperboloid manifold, denoted as \mathcal{L}^d , with a constant negative curvature, is defined as the Riemannian manifold (\mathbb{H}^d, g_{ℓ}) . Here, we adopt the constant negative curvature of -1 , and g_{ℓ} is the metric tensor represented by $\text{diag}([-1, 1, \dots, 1])$, and \mathbb{H}^d is the set of all vectors $\mathbf{x} \in \mathbb{R}^{d+1}$ satisfying $\langle \mathbf{x}, \mathbf{x} \rangle_{\mathcal{L}} = -1$ and $x_0 > 0$.

Next, the corresponding intrinsic distance function for two points $\mathbf{x}, \mathbf{y} \in \mathcal{L}^d$ is provided as:

$$d_{\mathcal{L}}(\mathbf{x}, \mathbf{y}) = \text{arcosh}(-\langle \mathbf{x}, \mathbf{y} \rangle_{\mathcal{L}}). \quad (1)$$

Definition 3.3 (Tangent Space). For a point $\mathbf{x} \in \mathcal{L}^d$, the tangent space $\mathcal{T}_{\mathbf{x}}\mathcal{L}^d$ consists of all vectors \mathbf{v} that are orthogonal to \mathbf{x} under the Minkowski inner product. This orthogonality is defined such that $\langle \mathbf{x}, \mathbf{v} \rangle_{\mathcal{L}} = 0$. Therefore, the tangent space can be expressed as: $\mathcal{T}_{\mathbf{x}}\mathcal{L}^d = \{\mathbf{v} : \langle \mathbf{x}, \mathbf{v} \rangle_{\mathcal{L}} = 0\}$.

Definition 3.4 (Exponential and Logarithmic Maps). Let $\mathbf{x} \in \mathcal{L}^d$ and $\mathbf{v} \in \mathcal{T}_{\mathbf{x}}\mathcal{L}^d$. The exponential map $\exp_{\mathbf{x}} : \mathcal{T}_{\mathbf{x}}\mathcal{L}^d \rightarrow \mathcal{L}^d$ and the logarithmic map $\log_{\mathbf{x}} : \mathcal{L}^d \rightarrow \mathcal{T}_{\mathbf{x}}\mathcal{L}^d$ are defined as follows:

$$\exp_{\mathbf{x}}(\mathbf{v}) = \cosh(\|\mathbf{v}\|_{\mathcal{L}})\mathbf{x} + \sinh(\|\mathbf{v}\|_{\mathcal{L}})\frac{\mathbf{v}}{\|\mathbf{v}\|_{\mathcal{L}}}, \quad (2)$$

$$\log_{\mathbf{x}}(\mathbf{y}) = d_{\mathcal{L}}(\mathbf{x}, \mathbf{y})\frac{\mathbf{y} + \langle \mathbf{x}, \mathbf{y} \rangle_{\mathcal{L}}\mathbf{x}}{\|\mathbf{y} + \langle \mathbf{x}, \mathbf{y} \rangle_{\mathcal{L}}\mathbf{x}\|_{\mathcal{L}}}, \quad (3)$$

where $\|\mathbf{v}\|_{\mathcal{L}} = \sqrt{\langle \mathbf{v}, \mathbf{v} \rangle_{\mathcal{L}}}$ denotes the norm of \mathbf{v} in $\mathcal{T}_{\mathbf{x}}\mathcal{L}^d$.

For computational convenience, the origin of the hyperboloid manifold denoted as $\mathbf{o} = (1, 0, 0, \dots, 0)$ in \mathcal{L}^d , is selected as the reference point for the exponential and logarithmic maps. This choice allows for simplified expressions of these mappings.

$$\begin{aligned} \exp_{\mathbf{o}}(\mathbf{v}) &= \exp_{\mathbf{o}}\left(\begin{bmatrix} 0 \\ \mathbf{v}^E \end{bmatrix}\right) \\ &= \left(\cosh\left(\|\mathbf{v}^E\|_2\right), \sinh\left(\|\mathbf{v}^E\|_2\right)\frac{\mathbf{v}^E}{\|\mathbf{v}^E\|_2} \right), \end{aligned} \quad (4)$$

where the (\cdot) denotes concatenation and the \cdot^E denotes the embedding in Euclidean space [59].

3.2 Notations and Problem Statement

Notations. We denote a graph as $G = (\mathcal{V}, \mathcal{E})$, where \mathcal{V} is the set of nodes and \mathcal{E} is the set of edges. The topology (i.e., structure) information of G is represented by adjacency matrix $A \in \mathbb{R}^{n \times n}$, where n is the number of nodes. $A_{i,j} = 1$ if there is an edge between node v_i and v_j , otherwise, $A_{i,j} = 0$. We denote an attributed graph as $G = (\mathcal{V}, \mathcal{E}, \mathcal{X})$, where $\mathcal{X} \in \mathbb{R}^{n \times d_{attr}}$ represents the feature matrix of node features. Each row of \mathcal{X} represents a node's feature

vector with d_{attr} dimension. The graph set is denoted as $\mathcal{G} = \{G_1, G_2, \dots, G_m\}$, where m is the number of graphs in \mathcal{G} .

Problem Statement. In this work, we focus on the unsupervised graph-level anomaly detection task: in the training phase, we train the model only using normal graphs; in the inference phase, given a graph set \mathcal{G} containing normal graphs and anomalous graphs, HC-GLAD aims to distinguish anomalous graphs that are significantly different from normal graphs according to the anomaly score.

4 METHODOLOGY

In this section, we will introduce the dual hyperbolic contrastive learning for the unsupervised graph-level anomaly detection framework (namely, HC-GLAD). The overall framework and brief procedure are illustrated in Figure 3, and the pseudo-code is summarized in Algorithm 1.

4.1 Data Preprocessing

Graph Data Augmentation. We employ the perturbation-free graph augmentation strategy [22, 42] to generate two augmented views (i.e., v_1 and v_2) for an input graph G . Concretely, v_1 focuses more on attribute and is directly built by integrating the node attribute \mathcal{X} (for attributed graph) and adjacency matrix A . v_2 focuses more on structure and is built by structural encodings from the graph topology and then it is combined with adjacency matrix A .

Hypergraph Construction. After obtaining two augmented views of a graph, we essentially have two augmented graphs. Inspired by [18, 55], we leverage ternary relationships between nodes, named the "gold motif" (i.e., the triangular relationships formed by three nodes), which is fundamental and ubiquitous in network structures, to initially construct hypergraphs. Given the adjacency matrix A of an augmented graph, we first construct the relationship matrix $A_{relation}$ of the constructed hypergraph by using the gold motifs. It can be calculated by:

$$A_{relation} = (AA^T) \odot A = (AA) \odot A, \quad (5)$$

where $A^T = A$ because graph G is an undirected graph and A is symmetric.

We determine the high-order relationships between vertices based on the matrix $\hat{A}_{relation} = A_{relation} + I_N$, where I_N is the identity matrix. We further build the incidence matrix \mathbf{H}_{inc} , where if vertex v_i is connected by hyperedge ϵ , $H_{inc(i\epsilon)} = 1$, otherwise 0. While thoroughly investigating and utilizing the gold motifs, we must also consider instances that do not constitute this kind of high-order relationship and ensure the integrity of the entire graph. Therefore, we will also include the edges that are not part of the high-order relationships in the incidence matrix \mathbf{H}_{inc} . Finally, we get a hypergraph *HyperG* with N vertices and M hyperedges. The high-order relationships in hypergraph *HyperG* could be simply represented by the incidence matrix $\mathbf{H}_{inc} \in \mathbb{R}^{N \times M}$.

4.2 Hyperbolic (Hyper-)Graph Convolution

Before we conduct hyperbolic (hyper-)graph convolution, we insert a value 0 in the zeroth dimension of the Euclidean state of the node for both view v_1 and v_2 . Refer to Eq. (4), the initial hyperbolic node state \mathbf{e}^0 could be obtained by:

$$\mathbf{e}_i^0 = \exp_{\mathbf{o}}([0, \mathbf{x}_i]), \quad (6)$$

where \mathbf{x} is the initial feature (or encoding) from augmented graphs (i.e., v_1 and v_2). $[0, \mathbf{x}]$ denotes the operation of inserting the value 0 into the zeroth dimension of \mathbf{x} so that $[0, \mathbf{x}]$ could always be in the tangent space of origin [41, 50]. The superscript 0 in e_i^0 indicates the initial hyperbolic state.

4.2.1 Hyperbolic Graph Aggregation. Following [41, 50], we first map the initial embedding e_i^0 in hyperbolic space to the tangent space using the logarithmic map. Then, we select GCN as our fundamental graph encoder to perform graph convolution aggregation. The propagation rule in the l -th layer on the view v_1 can be expressed as:

$$\mathbf{H}_{graph}^{(v_1, l)} = \sigma \left(\hat{\mathbf{D}}^{-\frac{1}{2}} \hat{\mathbf{A}} \hat{\mathbf{D}}^{-\frac{1}{2}} \mathbf{H}_{graph}^{(v_1, l-1)} \mathbf{W}^{(l-1)} \right), \quad (7)$$

where $\hat{\mathbf{A}} = \mathbf{A} + \mathbf{I}_N$ is the adjacency matrix \mathbf{A} of the input graph G_i with added self-connections, and \mathbf{I}_N is the identity matrix. $\hat{\mathbf{D}}$ is the degree matrix, $\mathbf{H}^{(v_1, l-1)}$ is node embedding matrix in the $(l-1)$ -th layer of view v_1 , $\mathbf{W}^{(l-1)}$ is a layer-specific trainable weight matrix, and $\sigma(\cdot)$ is a non-linear activation function [17]. The calculation of view v_2 can be calculated in the same way. After we obtain the final embedding \mathbf{h}_i^l of node i in tangent space, we map the final embedding from tangent space to hyperbolic space using the exponential map.

4.2.2 Hyperbolic Hypergraph Aggregation. Similar to hyperbolic graph aggregation, we first map the initial embedding e_i^0 in hyperbolic space to the tangent space using the logarithmic map, then we employ HGCN as our fundamental hypergraph encoder to perform hypergraph convolution aggregation. The propagation rule in the l -th layer on the view v_1 can be expressed as:

$$\mathbf{H}_{hyperg}^{(v_1, l)} = \sigma(\mathbf{D}_{hyperg}^{-1/2} \mathbf{H}_{inc} \mathbf{W} \mathbf{B}^{-1} \mathbf{H}_{inc}^T \mathbf{D}_{hyperg}^{-1/2} \mathbf{H}_{hyperg}^{(v_1, l-1)} \mathbf{P}), \quad (8)$$

where $\mathbf{D}_{hyperg} \in \mathbb{R}^{N \times N}$ is the vertex degree matrix, $\mathbf{B} \in \mathbb{R}^{M \times M}$ is the hyperedge degree matrix, $\mathbf{W} \in \mathbb{R}^{M \times M}$ is the hyperedge weights matrix, $\mathbf{P} \in \mathbb{R}^{F^{(l-1)} \times F^{(l)}}$ is weight matrix between the $(l-1)$ -th and l -th layer [4]. The calculation of view v_2 can be calculated in the same way. After we obtain the final embedding \mathbf{h}_i^l of node i in tangent space, we map the final embedding from tangent space to hyperbolic space using the exponential map.

4.3 Multi-Level Contrast

Following [19, 22], we design a contrastive strategy considering both node-level and graph-level contrast to train the model. Our proposed model comprises both graph- and hypergraph-channels, and their methods for computing multi-level contrast are similar. We elaborate on this as follows through graph-channel contrast.

Node-level Contrast. For an input graph G_i , we first map node embedding into node-level contrast space with MLP-based projection head, and then we construct node-level contrastive loss to maximize the agreement between the embeddings belonging to different views on the node level:

$$\mathcal{L}_{node} = \frac{1}{|\mathcal{B}|} \sum_{G_j \in \mathcal{B}} \frac{1}{2|\mathcal{V}_{G_j}|} \sum_{v_i \in \mathcal{V}_{G_j}} \left[l(\mathbf{h}_i^{(v_1)}, \mathbf{h}_i^{(v_2)}) + l(\mathbf{h}_i^{(v_2)}, \mathbf{h}_i^{(v_1)}) \right], \quad (9)$$

Algorithm 1: HC-GLAD

Input : Graph set: $\mathcal{G} = \{G_1, G_2, \dots, G_m\}$;
Output : The anomaly scores for each graph $Score_G$;
Initialize: (i) graph data augmentation: Obtain two augmented graphs (i.e., v_1 and v_2) using perturbation-free graph augmentation strategy [22, 42]; (ii) hypergraph construction: Construct hypergraph by pre-designed gold motifs.

- 1 **Training Phase for** $i = 1$ to s_epochs **do**
- 2 Obtain initial hyperbolic node state e^0 by Eq. (6).
- 3 Hyperbolic graph aggregation.
- 4 Hyperbolic hypergraph Aggregation.
- 5 Graph-channel:
- 6 (i) conduct node-level contrast by Eq. (9);
- 7 (ii) conduct graph-level contrast by Eq. (11).
- 8 Hypergraph-channel:
- 9 (i) conduct node-level contrast by Eq. (9);
- 10 (ii) conduct graph-level contrast by Eq. (11).
- 11 Calculate graph-channel loss by Eq. (13).
- 12 Calculate hypergraph-channel loss similarly to the way to calculate graph-channel loss.
- 13 Calculate the total loss by Eq. (14).
- 14 **end**
- 15 **Inference Phase for** G_i in Graph set G **do**
- 16 Calculate anomaly scores by Eq. (15).
- 17 **end**

$$l(\mathbf{h}_i^{(v_1)}, \mathbf{h}_i^{(v_2)}) = -\log \frac{e^{(-H_{Dist}(\mathbf{h}_i^{(v_1)}, \mathbf{h}_i^{(v_2)})/\tau)}}{\sum_{v_k \in \mathcal{V}_{G_j} \setminus v_i} e^{(-H_{Dist}(\mathbf{h}_i^{(v_1)}, \mathbf{h}_k^{(v_2)})/\tau)}}. \quad (10)$$

In Eq. (9), \mathcal{B} is the training/testing batch and \mathcal{V}_{G_j} is the node set of graph G_j . The calculation of $l(\mathbf{h}_i^{(v_2)}, \mathbf{h}_i^{(v_1)})$ and $l(\mathbf{h}_i^{(v_1)}, \mathbf{h}_i^{(v_2)})$ is the same, and we briefly show the calculation of $l(\mathbf{h}_i^{(v_1)}, \mathbf{h}_i^{(v_2)})$ in Eq. (10). In Eq. (10), the $H_{Dist}(\cdot, \cdot)$ is the function to measure the hyperbolic distance between different views. In this work, we compute the distance as Eq. (1) indicates.

Graph-level Contrast. To obtain graph embedding \mathbf{h}_{G_i} of graph G_i , we employ the pooling operation simply on embeddings of nodes in graph G_i . We first map graph embedding into graph-level contrast space with an MLP-based projection head. Similar to the node-level loss \mathcal{L}_{node} , we then construct a graph-level loss for mutual agreement maximization on the graph level:

$$\mathcal{L}_{graph} = \frac{1}{2|\mathcal{B}|} \sum_{G_i \in \mathcal{B}} \left[l(\mathbf{h}_{G_i}^{(v_1)}, \mathbf{h}_{G_i}^{(v_2)}) + l(\mathbf{h}_{G_i}^{(v_2)}, \mathbf{h}_{G_i}^{(v_1)}) \right], \quad (11)$$

$$l(\mathbf{h}_{G_i}^{(v_1)}, \mathbf{h}_{G_i}^{(v_2)}) = -\log \frac{e^{(-H_{Dist}(\mathbf{h}_{G_i}^{(v_1)}, \mathbf{h}_{G_i}^{(v_2)})/\tau)}}{\sum_{G_j \in \mathcal{B} \setminus G_i} e^{(-H_{Dist}(\mathbf{h}_{G_i}^{(v_1)}, \mathbf{h}_{G_j}^{(v_2)})/\tau)}}, \quad (12)$$

where notations are similar to node-level loss, and $l(\mathbf{h}_{G_i}^{(v_2)}, \mathbf{h}_{G_i}^{(v_1)})$ is calculated in the same way as $l(\mathbf{h}_{G_i}^{(v_1)}, \mathbf{h}_{G_i}^{(v_2)})$. The training loss function on the graph channel is:

$$\mathcal{L}_{graph-channel} = \xi_1 \mathcal{L}_{node} + \xi_2 \mathcal{L}_{graph}, \quad (13)$$

where ξ_1 and ξ_2 are trade-off parameters, and we set $\xi_1 = 1$ and $\xi_2 = 1$ on experiments of this work for simplicity. The training loss function on the hypergraph channel is calculated in the same way as the one on the graph channel. Therefore, in the training phase,

Table 1: The hyperbolicity δ and average hyperbolicity δ_{avg} of datasets.

Dataset	PROTEINS_full	ENZYMES	AIDS	DHFR	BZR	COX2	DD	REDDIT-B	HSE	MMP	p53	PPAR-gamma	IMDB-B
δ	1.09	1.15	0.74	1.01	1.11	1.00	3.74	0.97	0.76	0.77	0.78	0.77	0.24
δ_{avg}	0.14	0.15	0.15	0.12	0.18	0.09	0.64	0.05	0.12	0.12	0.12	0.12	0.02

Table 2: The performance comparison in terms of AUC (in percent, mean value \pm standard deviation). The best performance is highlighted in **bold, and the second-best performance is underlined. †: we report the result from [22].**

Method	PK-OCSVM†	PK-iF†	WL-OCSVM†	WL-iF†	InfoGraph-iF†	GraphCL-iF†	OCGIN†	GLocalKD†	GOOD-D†	HC-GLAD
PROTEINS-full	50.49±4.92	60.70±2.55	51.35±4.35	61.36±2.54	57.47±3.03	60.18±2.53	70.89±2.44	<u>77.30±5.15</u>	71.97±3.86	77.51±2.58
ENZYMES	53.67±2.66	51.30±2.01	55.24±2.66	51.60±3.81	53.80±4.50	53.60±4.88	58.75±5.98	61.39±8.81	<u>63.90±3.69</u>	65.39±6.23
AIDS	50.79±4.30	51.84±2.87	50.12±3.43	61.13±0.71	70.19±5.03	79.72±3.98	78.16±3.05	93.27±4.19	<u>97.28±0.69</u>	99.51±0.38
DHFR	47.91±3.76	52.11±3.96	50.24±3.13	50.29±2.77	52.68±3.21	51.10±2.35	49.23±3.05	56.71±3.57	62.67±3.11	61.43±4.27
BZR	46.85±5.31	55.32±6.18	50.56±5.87	52.46±3.30	63.31±8.52	60.24±5.37	65.91±1.47	69.42±7.78	<u>75.16±5.15</u>	75.75±9.11
COX2	50.27±7.91	50.05±2.06	49.86±7.43	50.27±0.34	53.36±8.86	52.01±3.17	53.58±5.05	59.37±12.67	62.65±8.14	59.98±7.44
DD	48.30±3.98	71.32±2.41	47.99±4.09	70.31±1.09	55.80±1.77	59.32±3.92	72.27±1.83	80.12±5.24	73.25±3.19	<u>77.66±1.73</u>
REDDIT-B	45.68±2.24	46.72±3.42	49.31±2.33	48.26±0.32	68.50±5.56	71.80±4.38	75.93±8.65	77.85±2.62	88.67±1.24	<u>79.09±2.52</u>
HSE	57.02±8.42	56.87±10.51	62.72±10.13	53.02±5.12	53.56±3.98	51.18±2.71	<u>64.84±4.70</u>	59.48±1.44	69.65±2.14	64.05±4.75
MMP	46.65±6.31	50.06±3.73	55.24±3.26	52.68±3.34	54.59±2.01	54.54±1.86	71.23±0.16	67.84±0.59	70.51±1.56	<u>70.96±4.45</u>
p53	46.74±4.88	50.69±2.02	54.59±4.46	50.85±2.16	52.66±1.95	53.29±2.32	58.50±0.37	<u>64.20±0.81</u>	62.99±1.55	66.01±1.77
PPAR-gamma	53.94±6.94	45.51±2.58	57.91±6.13	49.60±0.22	51.40±2.53	50.30±1.56	71.19±4.28	64.59±0.67	67.34±1.71	<u>69.51±5.04</u>
IMDB-B	50.75±3.10	50.80±3.17	54.08±5.19	54.08±5.19	56.50±3.58	56.50±4.90	60.19±8.90	52.09±3.41	65.88±0.75	<u>60.92±3.39</u>
Avg.Rank	8.77	7.85	7.15	7.77	6.15	6.54	3.77	3.31	<u>2.00</u>	1.69

we employ the loss function as:

$$\mathcal{L}_{total} = \lambda_1 \mathcal{L}_{graph-channel} + \lambda_2 \mathcal{L}_{hypergraph-channel}. \quad (14)$$

4.4 Anomaly Scoring

In the inference phase, we calculate the anomaly score from both graph-channel and hypergraph-channel, where a higher score indicates a greater anomaly. For simplicity and efficiency, we directly employ the \mathcal{L}_{total} (Eq. (14)) as the final anomaly score for an input graph G_i as:

$$score_{G_i} = \mathcal{L}_{total}. \quad (15)$$

5 EXPERIMENTS

5.1 Experimental Setup

Datasets. We conduct experiments on 13 open-source datasets from TUDataset [30], which involves small molecules, bioinformatics, and social networks. Appendix B.1 provides more details of the datasets. We follow the settings in [22, 27] to define anomaly, while the rest are viewed as normal data (i.e., normal graphs). Similar to [22, 27, 61], only normal data are utilized during the training phase.

To measure the hyperbolic nature in the datasets, we introduce the hyperbolicity δ proposed by Gromov [14]. In general, the hyperbolicity δ quantifies the tree-likeness of a graph. The lower the value of δ , the more tree-like the structure, suitable to embed in hyperbolic space [43]. When $\delta = 0$, the graph can be considered a tree [1, 53]. For more accuracy, we also report the average hyperbolicity δ_{avg} , which is robust to the addition or removal of an edge from the graph [59]. Given that the time complexity for calculating

δ and δ_{avg} is $O(n^4)$, we employ a random sampling method to approximate the calculations [7, 58, 59]. The results are illustrated in Table 1. Appendix B.2 explains the definition of hyperbolicity and shows the hyperbolicity distribution of the graph for some datasets in detail.

Baselines. We select 9 representative baselines from the non-end-to-end and end-to-end methods to compare with our proposed model. And for the non-end-to-end methods, we mainly select two categories: (i) kernel + detector. (ii) GCL model + detector.

- **Graph kernel + detector.** We adopt Weisfeiler-Lehman kernel (WL in short) [39] and propagation kernel (PK in short) [31] to first obtain representations, and then we take one-class SVM (OCSVM in short) [29] and isolation forest (iF in short) [20] to detect anomaly. After arranging and combining the above kernels and detectors, there are four baselines available: PK-OCSVM, PK-iF, WL-OCSVM, and WL-iF.
- **GCL model + detector.** Considering that we used the paradigm of graph contrastive learning, we select two classic graph-level contrastive learning models (i.e., InfoGraph [40] and GraphCL [54]) to first obtain representations, and then we take iF as detector to detect anomaly (i.e., InfoGraph-iF, GraphCL-iF).
- **End-to-end method.** We select 3 classical models: OCGIN [61], GLocalKD [27] and GOOD-D [22].

Metrics and Implementations. Following [19, 22, 26, 27], we adopt popular graph-level anomaly detection metric AUC (i.e., the area under the receiver operating characteristic) to evaluate methods. A higher AUC value corresponds to better anomaly detection

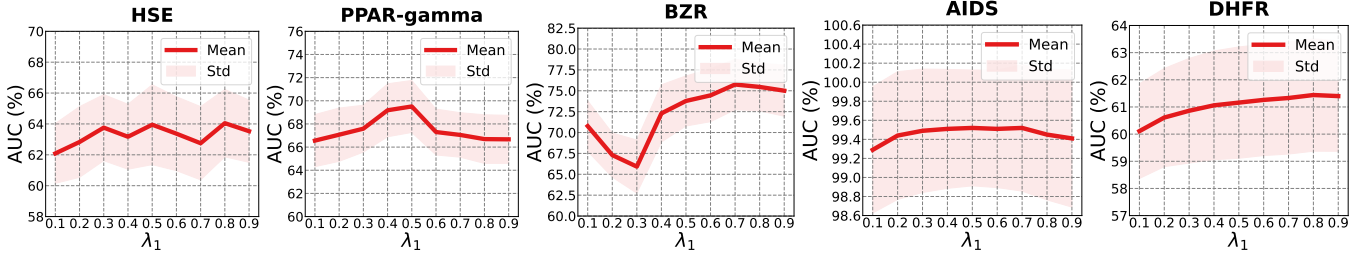


Figure 4: Hyper-parameter analysis (trade-off parameter λ_1) on representative datasets.

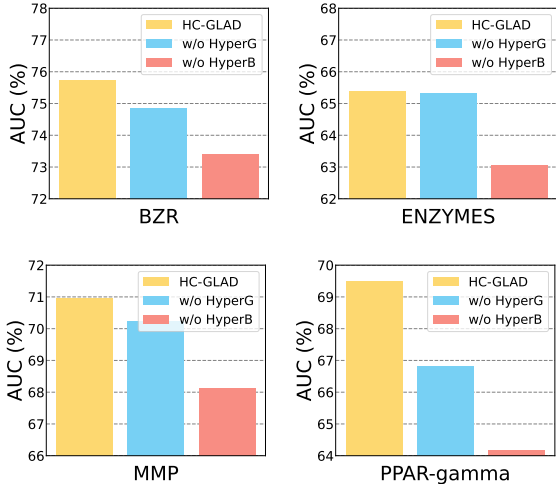


Figure 5: Ablation study on representative datasets.

performance. We use the Riemannian SGD with weight decay to learn the parameters of the network [5, 50]. In practice, we implement HC-GLAD with PyTorch [35].

5.2 Overall Performance

The AUC results of HC-GLAD, along with nine other baseline methods, are summarized in Table 2. As depicted in Table 2, HC-GLAD outperforms other methods by securing first place on 5 datasets and second place on 7 datasets, while maintaining a competitive performance on the remaining dataset. Furthermore, HC-GLAD achieves the best average rank among all methods across the 13 datasets. Our observations indicate that graph kernel-based methods exhibit the poorest performance among baselines. This underperformance is attributed to their limited ability to identify regular patterns and essential graph information, rendering them less effective with complex datasets. GCL-based methods show a moderate level of performance, highlighting the competitive potential of graph contrastive learning for UGAD tasks. In conclusion, the competitive performance of our proposed model underscores the effectiveness of incorporating node group information, as well as integrating hypergraph learning and hyperbolic geometry into graph-level anomaly detection. These findings also validate that HC-GLAD possesses inherent capabilities to capture fundamental characteristics of normal graphs, consequently delivering superior anomaly detection performance.

Table 3: The AUC (%) performance comparison of different motifs for hypergraph construction.

Dataset	ENZYMES	COX2	PPAR-gamma	p53	BZR	MMP
Triangle Variant	64.23	57.66	68.71	65.49	75.51	70.27
Triangle (Ours)	65.39	59.98	69.51	66.01	75.75	70.96

5.3 Ablation Study

We conduct an ablation study on four representative datasets to investigate the effects of the two key components: hypergraph-channel and hyperbolic learning. For convenience, let *w/o HyperG* and *w/o HyperB* denote the customized variants of HC-GLAD without hypergraph-channel and hyperbolic learning, respectively. As shown in Figure 5, we can observe that HC-GLAD consistently achieves the best performance against two variants, demonstrating that hypergraph learning and hyperbolic learning are necessary to get the best detection performance. Compared with HC-GLAD, the poor performance of *w/o HyperG* proves the importance of considering node group information and introducing hypergraph learning to this field. The poor performance of *w/o HyperB* proves the importance of introducing hyperbolic learning to UGAD. Additionally, we find that on these datasets, hyperbolic learning has a more pronounced impact compared to hypergraph learning.

5.4 Hypergraph Motifs Impact

To further evaluate the effectiveness of using the triangular relationship as the “gold motif” for hypergraph construction, we conduct an additional experiment by modifying the motif structure. Specifically, instead of using a complete triangle, we remove one edge from the triangle as a triangle variant to analyze the impact of different motif structures. Table 3 shows a consistent decline in AUC performance across all six datasets. That indicates that a complete triangle captures essential high-order correlations between nodes, which are critical for anomaly detection. With an acceptable computational overhead, the triangle motif provides a more comprehensive and robust representation of the hypergraph.

5.5 Hyper-parameter Analysis

Trade-off parameter λ_1 . In \mathcal{L}_{total} in Eq. (14), λ_1 and λ_2 are trade-off parameters that determine weights of the graph-channel and hypergraph-channel, respectively. To investigate their impact on model performance, we conduct experiments on representative datasets as shown in Figure 4. For simplicity, we set $\lambda_2 = 1 - \lambda_1$. We observe that as λ_1 increases from 0.1 to 0.9, the performance trend varies across different datasets. However, its variation does not

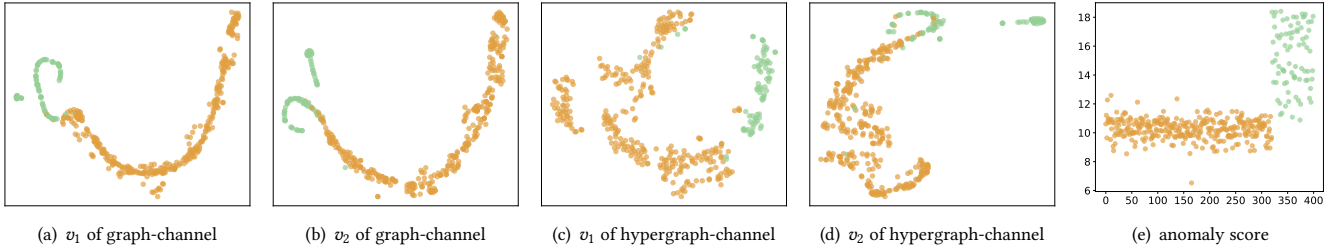


Figure 6: Visualization on AIDS dataset for different view v_1 and v_2 . (• denotes normal graph, • denotes anomalous graph.)

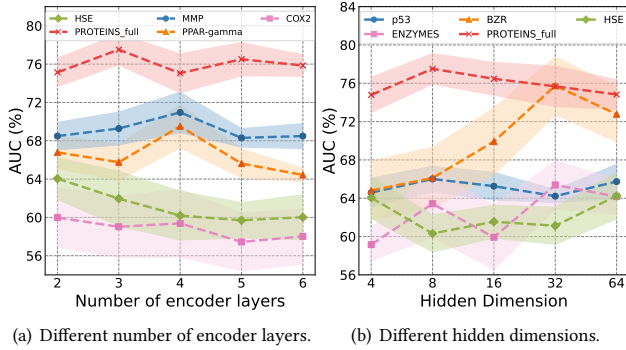


Figure 7: AUC (%) performance w.r.t. the number of encoder layers and hidden dimensions on representative datasets.

significantly affect model performance, indicating relative stability and high robustness of the proposed model.

The Number of Encoder Layers. To investigate the impact of encoder layers on model performance, we conduct experiments on five representative datasets as shown in Figure 7(a). We observe that when the number of layers is set to 3 or 4, the model exhibits promising performance. However, increasing more layers yields no significant performance improvements. When the number of layers reaches 6, a phenomenon of performance degradation commonly occurs, which we attribute to over-smoothing.

Hidden Dimension. We also investigate the impact of hidden dimensions on model performance through experiments on five datasets as shown in Figure 7(b). Based on our observations, we can preliminarily conclude that a higher dimension does not necessarily improve performance. In certain intervals, increasing the dimension can actually degrade the model’s performance. The impact of dimension change on model performance is minimal across most datasets, with the model performance remaining relatively stable.

To further explore the impact of hidden dimensions on model performance in hyperbolic and Euclidean space, we conduct additional experiments on two representative datasets using our model HC-GLAD and its variant, *w/o HyperB* (where the embedding learning is performed in Euclidean space). As shown in Figure 8, HC-GLAD in hyperbolic space consistently outperforms the *w/o HyperB* in Euclidean space across all hidden dimensions. And the performance gap between the two models narrows with increasing hidden dimension. However, the computational overhead also grows accordingly. These findings further validate the superiority of hyperbolic space for representation.

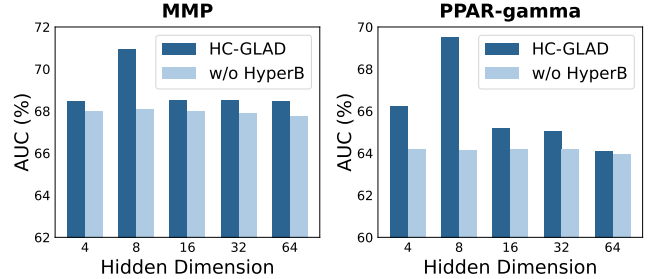


Figure 8: The effect of hidden dimension on HC-GLAD (hyperbolic model) and *w/o HyperB* (Euclidean model) performance in terms of AUC.

5.6 Visualization

To better understand our proposed model, we employ T-SNE [44] to visualize the embeddings learned by HC-GLAD on AIDS dataset as shown in Figure 6. The graph embeddings of view v_1 and v_2 , learned via the graph-channel or hypergraph-channel, successfully differentiate most normal graphs from anomalous ones, demonstrating the strong representational capacity of our framework. However, certain subtle anomalies remain harder to detect, indicating that relying solely on one channel or view may still miss more nuanced distinctions. It is ultimately the mechanism designed by HC-GLAD that distinctly differentiates normal graphs from anomalous graphs. This demonstrates the effectiveness of our scoring mechanism.

6 CONCLUSION

In this paper, we propose a novel framework named HC-GLAD, which integrates the strength of hypergraph learning and hyperbolic learning to jointly enhance the performance of UGAD. In concrete, we employ hypergraph learning built on gold motifs to exploit the node group information and utilize hyperbolic geometry to explore the latent hierarchical information. To the best of our knowledge, this is the first work to simultaneously introduce hypergraph exploiting node group information and hyperbolic geometry to the UGAD task. Through extensive experiments, we validate the superiority of HC-GLAD on 13 real-world datasets corresponding to different fields. One limitation of our method is that the integration of multiple learning paradigms in our framework may introduce increased computational cost. A more detailed time complexity analysis can be found in Appendix B.3. In the future, we will explore the design of lightweight yet efficient frameworks to overcome this limitation.

REFERENCES

- [1] Réka Albert, Bhaskar DasGupta, and Nasim Mobasher. 2014. Topological implications of negative curvature for biological and social networks. *Phys. Rev. E* 89 (Mar 2014), 032811. Issue 3. <https://doi.org/10.1103/PhysRevE.89.032811>
- [2] Alessia Antelmi, Gennaro Cordasco, Mirko Polato, Vittorio Scarano, Carmine Spagnuolo, and Dingqi Yang. 2023. A survey on hypergraph representation learning. *Comput. Surveys* 56, 1 (2023), 1–38.
- [3] Gregor Bachmann, Gary Bécigneul, and Octavian Ganea. 2020. Constant curvature graph convolutional networks. In *International conference on machine learning*. PMLR, 486–496.
- [4] Song Bai, Feihu Zhang, and Philip HS Torr. 2021. Hypergraph convolution and hypergraph attention. *Pattern Recognition* 110 (2021), 107637.
- [5] Silvere Bonnabel. 2013. Stochastic gradient descent on Riemannian manifolds. *IEEE Trans. Automat. Control* 58, 9 (2013), 2217–2229.
- [6] Joey Bose, Ariella Smofsky, Renjie Liao, Prakash Panangaden, and Will Hamilton. 2020. Latent variable modelling with hyperbolic normalizing flows. In *International Conference on Machine Learning*. PMLR, 1045–1055.
- [7] Ines Chami, Zitao Ying, Christopher Ré, and Jure Leskovec. 2019. Hyperbolic graph convolutional neural networks. *Advances in neural information processing systems* 32 (2019).
- [8] Fangying Chen, Junyoung Park, and Jinkyoo Park. 2021. A Molecular Hypermessage Passing Network with Functional Group Information. *arXiv preprint arXiv:2106.01028* (2021).
- [9] Junwu Chen and Philippe Schwaller. 2024. Molecular hypergraph neural networks. *The Journal of Chemical Physics* 160, 14 (2024).
- [10] Yifan Feng, Haoxuan You, Zizhao Zhang, Rongrong Ji, and Yue Gao. 2019. Hypergraph neural networks. In *Proceedings of the AAAI conference on artificial intelligence*, Vol. 33. 3558–3565.
- [11] Xingcheng Fu, Yucen Wei, Qingyun Sun, Haonan Yuan, Jia Wu, Hao Peng, and Jianxin Li. 2023. Hyperbolic geometric graph representation learning for hierarchy-imbalance node classification. In *Proceedings of the ACM Web Conference 2023*. 460–468.
- [12] Yue Gao, Yifan Feng, Shuyi Ji, and Rongrong Ji. 2022. HGNN+: General hypergraph neural networks. *IEEE Transactions on Pattern Analysis and Machine Intelligence* 45, 3 (2022), 3181–3199.
- [13] Yue Gao, Zizhao Zhang, Haojie Lin, Xibin Zhao, Shaoyi Du, and Changqing Zou. 2022. Hypergraph Learning: Methods and Practices. *IEEE transactions on pattern analysis and machine intelligence* 44, 5 (2022), 2548–2566.
- [14] M. Gromov. 1987. *Hyperbolic Groups*. Springer New York, New York, NY, 75–263. https://doi.org/10.1007/978-1-4613-9586-7_3
- [15] Jiadi Han, Qian Tao, Yufei Tang, and Yuhua Xia. 2022. DH-HGCN: dual homogeneity hypergraph convolutional network for multiple social recommendations. In *Proceedings of the 45th international ACM SIGIR conference on research and development in information retrieval*. 2190–2194.
- [16] Shuyi Ji, Yifan Feng, Rongrong Ji, Xibin Zhao, Wanwan Tang, and Yue Gao. 2020. Dual channel hypergraph collaborative filtering. In *Proceedings of the 26th ACM SIGKDD international conference on knowledge discovery & data mining*. 2020–2029.
- [17] Thomas N Kipf and Max Welling. 2016. Semi-supervised classification with graph convolutional networks. *arXiv preprint arXiv:1609.02907* (2016).
- [18] Geon Lee, Jihoon Ko, and Kijung Shin. 2020. Hypergraph motifs: concepts, algorithms, and discoveries. *arXiv preprint arXiv:2003.01853* (2020).
- [19] Jindong Li, Qianli Xing, Qi Wang, and Yi Chang. 2023. CVTGAD: Simplified Transformer with Cross-View Attention for Unsupervised Graph-Level Anomaly Detection. In *Joint European Conference on Machine Learning and Knowledge Discovery in Databases*. Springer, 185–200.
- [20] Fei Tony Liu, Kai Ming Ting, and Zhi-Hua Zhou. 2008. Isolation forest. In *2008 eighth IEEE international conference on data mining*. IEEE, 413–422.
- [21] Qi Liu, Maximilian Nickel, and Douwe Kiela. 2019. Hyperbolic graph neural networks. *Advances in neural information processing systems* 32 (2019).
- [22] Yixin Liu, Kaize Ding, Huan Liu, and Shirui Pan. 2023. Good-d: On unsupervised graph out-of-distribution detection. In *Proceedings of the Sixteenth ACM International Conference on Web Search and Data Mining*. 339–347.
- [23] Yixin Liu, Kaize Ding, Qinghua Lu, Fuyi Li, Leo Yu Zhang, and Shirui Pan. 2024. Towards self-interpretable graph-level anomaly detection. *Advances in Neural Information Processing Systems* 36 (2024).
- [24] Yixin Liu, Ming Jin, Shirui Pan, Chuan Zhou, Yu Zheng, Feng Xia, and S Yu Philip. 2022. Graph self-supervised learning: A survey. *IEEE transactions on knowledge and data engineering* 35, 6 (2022), 5879–5900.
- [25] Yixin Liu, Yizhen Zheng, Daokun Zhang, Vincent Lee, and Shirui Pan. 2023. Beyond Smoothing: Unsupervised Graph Representation Learning with Edge Heterophily Discriminating. In *Proceedings of the AAAI conference on artificial intelligence*.
- [26] Xuexiong Luo, Jia Wu, Jian Yang, Shan Xue, Hao Peng, Chuan Zhou, Hongyang Chen, Zhao Li, and Quan Z Sheng. 2022. Deep graph level anomaly detection with contrastive learning. *Scientific Reports* 12, 1 (2022), 19867.
- [27] Rongrong Ma, Guansong Pang, Ling Chen, and Anton van den Hengel. 2022. Deep graph-level anomaly detection by glocal knowledge distillation. In *Proceedings of the fifteenth ACM international conference on web search and data mining*. 704–714.
- [28] Xiaoxiao Ma, Jia Wu, Shan Xue, Jian Yang, Chuan Zhou, Quan Z Sheng, Hui Xiong, and Leman Akoglu. 2021. A comprehensive survey on graph anomaly detection with deep learning. *IEEE Transactions on Knowledge and Data Engineering* 35, 12 (2021), 12012–12038.
- [29] Larry M Manevitz and Malik Yousef. 2001. One-class SVMs for document classification. *Journal of machine Learning research* 2, Dec (2001), 139–154.
- [30] Christopher Morris, Nils M Kriege, Franka Bause, Kristian Kersting, Petra Mutzel, and Marion Neumann. 2020. TUDataset: A collection of benchmark datasets for learning with graphs. *arXiv preprint arXiv:2007.08663* (2020).
- [31] Marion Neumann, Roman Garnett, Christian Bauckhage, and Kristian Kersting. 2016. Propagation kernels: efficient graph kernels from propagated information. *Machine Learning* 102 (2016), 209–245.
- [32] Maximilian Nickel, Xueyan Jiang, and Volker Tresp. 2014. Reducing the rank in relational factorization models by including observable patterns. *Advances in Neural Information Processing Systems* 27 (2014).
- [33] Maximilian Nickel and Douwe Kiela. 2018. Learning continuous hierarchies in the lorentz model of hyperbolic geometry. In *International conference on machine learning*. PMLR, 3779–3788.
- [34] Chaoxi Niu, Guansong Pang, and Ling Chen. 2023. Graph-level anomaly detection via hierarchical memory networks. In *Joint European Conference on Machine Learning and Knowledge Discovery in Databases*. Springer, 201–218.
- [35] Adam Paszke, Sam Gross, Francisco Massa, Adam Lerer, James Bradbury, Gregory Chanan, Trevor Killeen, Zeming Lin, Natalia Gimelshein, Luca Antiga, et al. 2019. Pytorch: An imperative style, high-performance deep learning library. *Advances in neural information processing systems* 32 (2019).
- [36] Chen Qiu, Marius Kloft, Stephan Mandt, and Maja Rudolph. 2022. Raising the Bar in Graph-level Anomaly Detection. In *International Joint Conference on Artificial Intelligence*.
- [37] Jiezhong Qiu, Qibin Chen, Yuxiao Dong, Jing Zhang, Hongxia Yang, Ming Ding, Kuansan Wang, and Jie Tang. 2020. Gcc: Graph contrastive coding for graph neural network pre-training. In *Proceedings of the 26th ACM SIGKDD international conference on knowledge discovery & data mining*. 1150–1160.
- [38] Erzsébet Ravasz and Albert-László Barabási. 2003. Hierarchical organization in complex networks. *Physical review E* 67, 2 (2003), 026112.
- [39] Nino Shervashidze, Pascal Schweitzer, Erik Jan Van Leeuwen, Kurt Mehlhorn, and Karsten M Borgwardt. 2011. Weisfeiler-lehman graph kernels. *Journal of Machine Learning Research* 12, 9 (2011).
- [40] Fan-Yun Sun, Jordon Hoffman, Vikas Verma, and Jian Tang. 2020. InfoGraph: Unsupervised and Semi-supervised Graph-Level Representation Learning via Mutual Information Maximization. In *International Conference on Learning Representations*.
- [41] Jianing Sun, Zhaoyue Cheng, Saba Zuberi, Felipe Pérez, and Maksims Volkovs. 2021. Hgcf: Hyperbolic graph convolution networks for collaborative filtering. In *Proceedings of the Web Conference 2021*. 593–601.
- [42] Yue Tan, Yixin Liu, Guodong Long, Jing Jiang, Qinghua Lu, and Chengqi Zhang. 2023. Federated learning on non-iid graphs via structural knowledge sharing. In *Proceedings of the AAAI conference on artificial intelligence*, Vol. 37. 9953–9961.
- [43] Alexandru Tifrea, Gary Bécigneul, and Octavian-Eugen Ganea. 2019. Poincare Glove: Hyperbolic Word Embeddings. In *7th International Conference on Learning Representations, ICLR 2019, New Orleans, LA, USA, May 6–9, 2019*. OpenReview.net. <https://openreview.net/forum?id=Ske5r3AqK7>
- [44] Laurens Van der Maaten and Geoffrey Hinton. 2008. Visualizing data using t-SNE. *Journal of machine learning research* 9, 11 (2008).
- [45] Petar Velickovic, William Fedus, William L Hamilton, Pietro Liò, Yoshua Bengio, and R Devon Hjelm. 2019. Deep graph infomax. *ICLR (Poster)* 2, 3 (2019), 4.
- [46] Lirong Wu, Haitao Lin, Cheng Tan, Zhangyang Gao, and Stan Z Li. 2021. Self-supervised learning on graphs: Contrastive, generative, or predictive. *IEEE Transactions on Knowledge and Data Engineering* 35, 4 (2021), 4216–4235.
- [47] Lianghao Xia, Chao Huang, Yong Xu, Jiashu Zhao, Dawei Yin, and Jimmy Huang. 2022. Hypergraph contrastive collaborative filtering. In *Proceedings of the 45th International ACM SIGIR conference on research and development in information retrieval*. 70–79.
- [48] Keyulu Xu, Weihua Hu, Jure Leskovec, and Stefanie Jegelka. 2018. How powerful are graph neural networks? *arXiv preprint arXiv:1810.00826* (2018).
- [49] Naganand Yadati, Madhav Nimishakavi, Prateek Yadav, Vikram Nitin, Anand Louis, and Partha Talukdar. 2019. Hypergen: A new method for training graph convolutional networks on hypergraphs. *Advances in neural information processing systems* 32 (2019).
- [50] Menglin Yang, Zhihao Li, Min Zhou, Jiahong Liu, and Irwin King. 2022. Hicf: Hyperbolic informative collaborative filtering. In *Proceedings of the 28th ACM SIGKDD Conference on Knowledge Discovery and Data Mining*. 2212–2221.
- [51] Menglin Yang, Min Zhou, Zhihao Li, Jiahong Liu, Lujia Pan, Hui Xiong, and Irwin King. 2022. Hyperbolic graph neural networks: A review of methods and applications. *arXiv preprint arXiv:2202.13852* (2022).

- [52] Menglin Yang, Min Zhou, Jiahong Liu, Defu Lian, and Irwin King. 2022. HRCF: Enhancing collaborative filtering via hyperbolic geometric regularization. In *Proceedings of the ACM Web Conference 2022*. 2462–2471.
- [53] Menglin Yang, Min Zhou, Hui Xiong, and Irwin King. 2023. Hyperbolic Temporal Network Embedding. *IEEE Trans. Knowl. Data Eng.* 35, 11 (2023), 11489–11502. <https://doi.org/10.1109/TKDE.2022.3232398>
- [54] Yuning You, Tianlong Chen, Yongduo Sui, Ting Chen, Zhangyang Wang, and Yang Shen. 2020. Graph contrastive learning with augmentations. *Advances in neural information processing systems* 33 (2020), 5812–5823.
- [55] Junliang Yu, Hongzhi Yin, Jundong Li, Qinyong Wang, Nguyen Quoc Viet Hung, and Xiangliang Zhang. 2021. Self-supervised multi-channel hypergraph convolutional network for social recommendation. In *Proceedings of the web conference 2021*. 413–424.
- [56] Zhenyang Yu, Xinye Wang, Bingzhe Zhang, Zhaohang Luo, and Lei Duan. 2023. TUAf: Triple-Unit-Based Graph-Level Anomaly Detection with Adaptive Fusion Readout. In *International Conference on Database Systems for Advanced Applications*. Springer, 415–430.
- [57] Junwei Zhang, Min Gao, Junliang Yu, Lei Guo, Jundong Li, and Hongzhi Yin. 2021. Double-scale self-supervised hypergraph learning for group recommendation. In *Proceedings of the 30th ACM international conference on information & knowledge management*. 2557–2567.
- [58] Yiding Zhang, Xiao Wang, Chuan Shi, Xunqiang Jiang, and Yanfang Ye. 2021. Hyperbolic graph attention network. *IEEE Transactions on Big Data* 8, 6 (2021), 1690–1701.
- [59] Yiding Zhang, Xiao Wang, Chuan Shi, Nian Liu, and Guojie Song. 2021. Lorentzian graph convolutional networks. In *Proceedings of the web conference 2021*. 1249–1261.
- [60] Huan Zhao, Xiaogang Xu, Yangqiu Song, Dik Lun Lee, Zhao Chen, and Han Gao. 2018. Ranking users in social networks with higher-order structures. In *Proceedings of the AAAI Conference on Artificial Intelligence*, Vol. 32.
- [61] L Zhao and L Akoglu. 2021. On Using Classification Datasets to Evaluate Graph Outlier Detection: Peculiar Observations and New Insights. *Big Data* 11, 3 (2021), 151–180.
- [62] Lingxiao Zhao and Leman Akoglu. 2023. On using classification datasets to evaluate graph outlier detection: Peculiar observations and new insights. *Big Data* 11, 3 (2023), 151–180.
- [63] Yanqiao Zhu, Yichen Xu, Feng Yu, Qiang Liu, Shu Wu, and Liang Wang. 2021. Graph contrastive learning with adaptive augmentation. In *Proceedings of the Web Conference 2021*. 2069–2080.

A SUPPLEMENTARY RELATED WORK

A.1 Graph Contrastive Learning

Graph contrastive learning employs the principle of mutual information maximization to extract rich representations by optimizing instances with similar semantic content [24, 46]. This approach has gained widespread application for achieving outstanding performance in unsupervised graph representation learning [25, 37, 40, 45, 54, 63]. For example, GraphCL [54] proposes four types of data augmentations for graph-structured data to create pairs for contrastive learning. In the context of graph classification, InfoGraph [40] aims to maximize the mutual information between graph-level and substructure-level representations, with the latter being computed at various scales. Recent research has also applied graph contrastive learning to the field of graph-level anomaly detection. For instance, GLADC [26] captures both node-level and graph-level representations using a dual-graph encoder module within a contrastive learning framework. GOOD-D [22] detects anomalous graphs by identifying semantic inconsistencies across different granularities through a hierarchical contrastive learning framework. CVTGAD [19] similarly incorporates graph contrastive learning principles, utilizing transformer for unsupervised graph anomaly detection and explicitly accounting for co-occurrence between different views.

B SUPPLEMENT OF EXPERIMENTS

B.1 Datasets

More details about datasets we employed in our experiments are illustrated in Table 4.

B.2 Hyperbolicity

The hyperbolicity is based on the 4-node condition, a quadruple of distinct nodes n_1, n_2, n_3, n_4 in a graph. Let $\pi = (\pi_1, \pi_2, \pi_3, \pi_4)$ be a permutation of node indices 1, 2, 3, and 4, such that

$$\begin{aligned} S_{n_1, n_2, n_3, n_4} &= d(n_{\pi_1}, n_{\pi_2}) + d(n_{\pi_3}, n_{\pi_4}) \\ &\leq M_{n_1, n_2, n_3, n_4} = d(n_{\pi_1}, n_{\pi_3}) + d(n_{\pi_2}, n_{\pi_4}) \\ &\leq L_{n_1, n_2, n_3, n_4} = d(n_{\pi_1}, n_{\pi_4}) + d(n_{\pi_2}, n_{\pi_3}), \end{aligned} \quad (16)$$

where d is the shortest path length, and define

$$\delta^+ = \frac{L_{n_1, n_2, n_3, n_4} - M_{n_1, n_2, n_3, n_4}}{2}. \quad (17)$$

The worst-case hyperbolicity [14] is defined as the maximum value of δ^+ among all quadruples in the graph, i.e.,

$$\delta_{worst} = \max_{n_1, n_2, n_3, n_4} \{\delta^+\}. \quad (18)$$

The average hyperbolicity [1] is defined as the average value of δ^+ among all quadruples in the graph, i.e.,

$$\delta_{avg} = \frac{1}{\binom{n}{4}} \sum_{n_1, n_2, n_3, n_4} \{\delta^+\}, \quad (19)$$

where n is the number of nodes in the graph.

A graph \mathcal{G} is called δ -hyperbolic if $\delta_{worst}(\mathcal{G}) \leq \delta$ [1]. We adopt the aforementioned δ_{worst} as the hyperbolicity δ of the datasets, which to some extent reflects the underlying hyperbolic geometry of the graph.

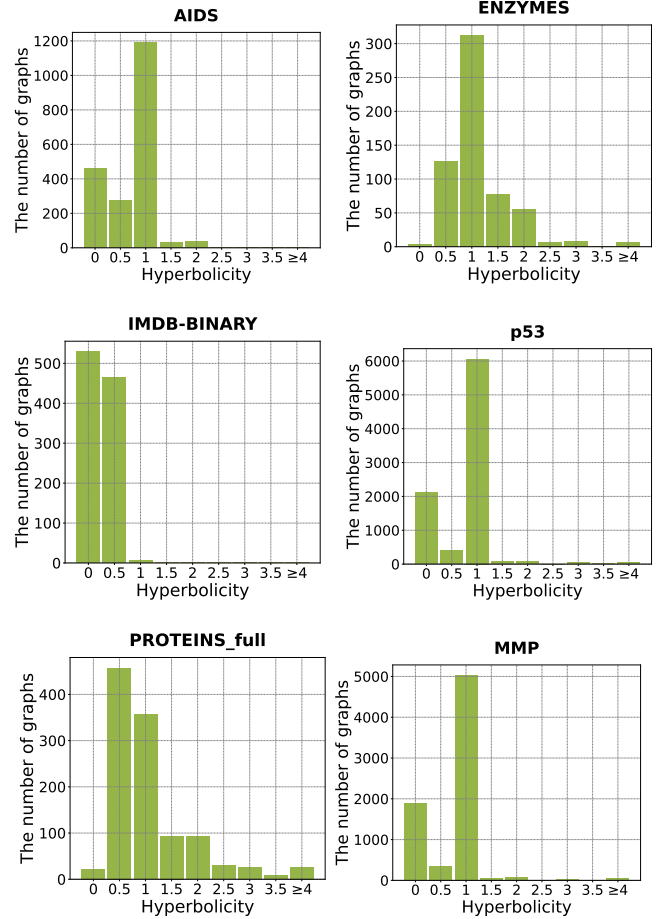


Figure 9: Hyperbolicity distribution in detail on representative datasets where the X-axis represents the hyperbolicity of the graph and the Y-axis represents the number of graphs with corresponding hyperbolicity values on the X-axis.

B.3 Time Complexity Analysis

While data augmentation follows the same standard process as [22], the hypergraph construction, whose core calculation is the Eq. (5), can be efficiently computed using sparse matrices [55, 60]. The data augmentation and hypergraph construction are both performed once during the preprocessing stage, and the time complexity of our model is mainly in the encoder and loss term. Let M denote the number of hyperedges, e denote the average number of edges, n denotes the average number of nodes, m denote the total number of graphs, \mathcal{B} denote the batch size, d denote latent embedding dimension, d_{in} denote the dimension of input-layer embedding and L denote the number of encoder layers. For the graph encoder GNN, the time complexity is $O(mLed + mLnd^2 + mndd_{in})$. For the hypergraph encoder HGCN, the time complexity is $O(mLMd + mLnd^2 + mMdd_{in})$. For node-level loss, the time complexity is $O(mn^2d)$. For graph-level loss, the time complexity is $O(m\mathcal{B}d)$. So our model’s time complexity is $O(mLd(e + nd + M) + md(nd_{in} + Md_{in} + n^2 + \mathcal{B}))$ for training, ignoring constant coefficient term and the smaller terms.

Table 4: The statistics of datasets of our experiments from TUDataset [30].

Dataset	PROTEINS_full	ENZYMES	AIDS	DHFR	BZR	COX2	DD	REDDIT-B	HSE	MMP	p53	PPAR-gamma	IMDB-B
Graphs	1113	600	2000	467	405	467	1178	2000	8417	7558	8903	8451	1000
Avg. Nodes	39.06	32.63	15.69	42.43	35.75	41.22	284.32	429.63	16.89	17.62	17.92	17.38	19.77
Avg. Edges	72.82	62.14	16.20	44.54	38.36	43.45	715.66	497.75	17.23	17.98	18.34	17.72	96.53